Clinical Imaging 41 (2016) 53–58

Contents lists available at ScienceDirect

Clinical Imaging

journal homepage: http://www.clinicalimaging.org

Differentiation of subtypes of renal cell carcinoma: dynamic contrast-enhanced magnetic resonance imaging versus diffusion-weighted magnetic resonance imaging☆

Akira Yamamoto *, Tsutomu Tamada, Katsuyoshi Ito, Teruki Sone, Akihiko Kanki, Daigo Tanimoto, Yasufumi Noda

Department of Radiology, Kawasaki Medical School, Kurashiki, Japan

ARTICLE INFO

Article history:
Received 2 June 2016
Received in revised form 16 September 2016
Accepted 3 October 2016
Available online xxxx

Keywords:
Renal cell carcinoma
Subtype
Diffusion-weighted imaging
Contrast-enhanced imaging

ABSTRACT

Objective: The objective was to compare the performance of dynamic contrast-enhanced (DCE) and diffusion-weighted (DW) magnetic resonance (MR) imaging in the differentiation of subtypes of renal cell carcinoma (RCC).
Materials/methods: This study included 45 renal tumors of clear cell (n=36) and non-clear-cell (n=9) RCC. The contrast enhancement ratios (CERs) and the apparent diffusion coefficient (ADC) values on MR imaging were compared between the clear cell and non-clear-cell RCC groups.
Results: In the comparison of diagnostic performance between DCE and DW MR imaging, areas under the curves were 0.968 and 0.797 for the CERs of the corticomedullary and the ADC value.
Conclusion: The CER of the corticomedullary phase was more reliable in distinguishing between clear cell and non-clear-cell RCCs.

1. Background

Renal cell carcinoma (RCC) is the most common primary malignant tumor of the kidney [1], with multiple subtypes. The most common subtypes of RCC are clear cell, papillary, and chromophobe, accounting for 70%–80%, 14%–17%, and 4%–8% of all RCCs, respectively [1–3]. These subtypes differ in their prognoses, with clear cell RCC known to have a relatively worse prognosis than papillary and chromophobe RCCs [4–6]. In addition, their responses to available targeted therapies differ. In patients with advanced and metastatic RCCs, the tyrosine kinase inhibitors sunitinib and sorafenib are more effective in patients with clear cell RCCs, whereas temsirolimus has recently been shown to be more effective against non-clear-cell RCCs [7–10]. Because of these differences in patient prognoses and responses to targeted therapies, accurate identification of the specific diagnosis prior to treatment is important.

Percutaneous biopsy of renal tumors has been widely demonstrated to be an accurate method of diagnosing preoperative pathologic subtypes in many patients [11–13]. However, the risk of procedural complications and the potential for sampling error have hindered universal acceptance of percutaneous biopsy [14–17].

Dynamic contrast-enhanced (DCE) computed tomography (CT) provides a useful method of differentiating clear cell RCC from non-clear-cell RCC since studies have shown that non-clear-cell RCC is a less vascularized lesion than clear cell RCC [18–20]. DCE magnetic resonance (MR) imaging with higher contrast resolution than CT demonstrates high accuracy in differentiating clear cell RCC from non-clear-cell RCC [21–23]. Sun et al. [23] reported that signal intensity (SI) changes of the corticomedullary phase on DCE MR imaging were the most effective parameter for distinguishing clear cell and papillary RCCs; a threshold value of 84% permitted distinction with 93% sensitivity and 96% specificity. More recent studies on renal tumors have shown that the apparent diffusion coefficient (ADC) value of diffusion-weighted (DW) MR imaging may provide a new quantitative method for diagnosing pathological subtypes of RCC [24–27]. Wang et al. [27] reported that ADC values of clear cell RCCs were significantly higher than those of papillary RCCs and chromophobe RCCs; a threshold value of 1.281×10^{-3} mm^2/s permitted distinction with 96% sensitivity and 94% specificity. However, there has been no report comparing these two MR imaging techniques in the same study. The purpose of this study was to compare the diagnostic performance of DCE MR imaging and DW MR imaging in the differentiation of subtypes of RCC (clear cell versus non-clear-cell RCC).

2. Methods

Our institutional review board approved this retrospective study, and the need to obtain informed consent was waived. This study was compliant with the Health Insurance Portability and Accounting Act.

☆ The authors have no conflict of interest to disclose.

* Corresponding author. Kawasaki Medical School, Department of Radiology, 577 Matsushima, Kurashiki, Okayama 701-0192, Japan. Tel.: +81 86 462 1111; fax: +81 86 462 1199.
E-mail address: jiro@med.kawasaki-m.ac.jp (A. Yamamoto).

http://dx.doi.org/10.1016/j.clinimag.2016.10.001
0899-7071/

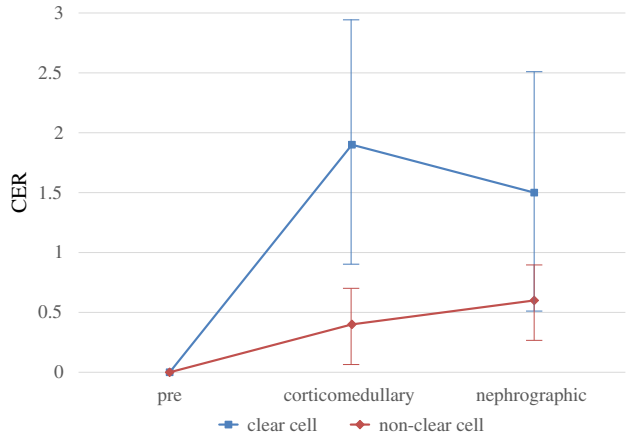

Fig. 1. Clear cell RCC shows a marked increase of CER in the corticomedullary phase, with a decrease in the nephrographic phase. Non-clear-cell RCC shows a gradual increase of CER from the corticomedullary phase to the nephrographic phase.

2.1. Patients

Our institution's pathology database was retrospectively searched to derive all histologically proven cases of RCC from March 2004 to December 2012. During the study period, 278 cases were histologically proven to be RCC, and of these, 48 patients underwent MR imaging including DCE MR imaging and DW MR imaging. Three cases were excluded from the study because of unclassified RCC (n=3). Finally, 45 renal lesions in 45 patients (30 men, 15 women; mean age, 62.6 years; age range, 18–88 years) were included in this study. Histopathologic analysis was performed on specimens acquired at radical (n=27) or partial (n=18) nephrectomy. The mean time interval between the MR imaging examination and the surgery was 32.0 days (range, 0–228 days). Pathologic diagnoses of the 45 RCCs included 36 clear cell RCCs, 9 non-clear-cell including 6 papillary RCCs, and 3 chromophobe RCCs. Not only solid lesions but also lesions with cystic degeneration and/or a necrotic component were included.

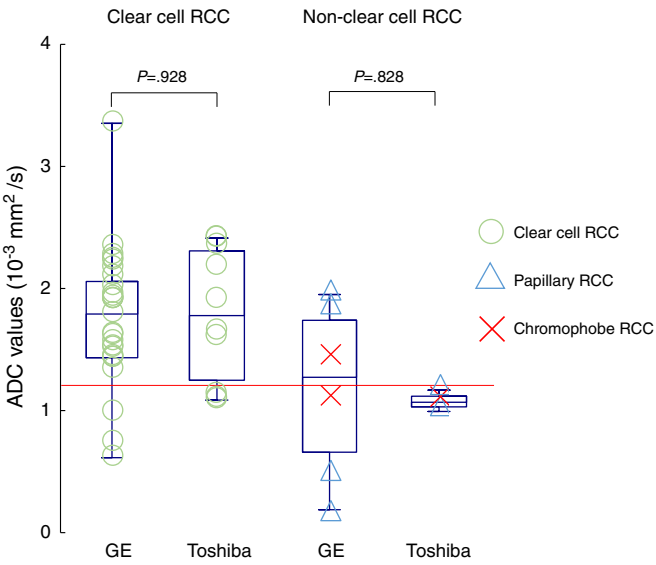

Fig. 2. The boxplots of ADC values of clear cell RCC and non-clear-cell RCC with each MR system with optimal threshold (1.2×10^{-3} mm^2/s) show no significant differences in the ADC values between the MR systems of GE and Toshiba in both clear cell RCC and non-clear-cell RCC. There is no bias in the distribution of chromophobe RCCs in the non-clear-cell RCCs.

Table 1
CER and ADC values of clear and non-clear-cell RCCs

Parameter	Clear cell RCC	Non-clear cell RCC	*P*
No. of tumors	36	9 (papillary 6, chromophobe 3)	
Tumor size (cm)	5.2±3.3	4.8±3.3	.753
CER in corticomedullary phase	1.9±0.9	0.4±0.3	<.001
CER in nephrographic phase	1.5±0.9	0.6±0.3	.001
ADC value ($\times10^{-3}$ mm^2/s)	1.8±0.5	1.1±0.6	.008

2.2. Imaging protocol

MR imaging was performed with two 1.5-T clinical MR systems (Signa Excite High Speed, GE Healthcare, Milwaukee, WI, or EXCELART Vantage Powered by Atlas, Toshiba Medical Systems, Tochigi, Japan) with a phased-array torso coil for signal reception. The routine renal MR imaging protocol included the following sequences: transverse and coronal breath-hold fast spoiled gradient-echo T1-weighted in-phase and opposed-phase imaging, transverse and coronal breath-hold fast spin-echo (FSE) T2-weighted imaging, single-shot FSE heavily T2-weighted imaging, and breath-hold fluid attenuated inversion recovery imaging. Transverse DW imaging was obtained using an SE single-shot echo-planar technique with free breathing for GE Healthcare [repetition time (TR)/echo time (TE), 5500/65.4 ms; flip angle, 90°; band width, 2604 Hz/pixel; signal averages, 8; field of view (FOV), 35 cm×35 cm; slice thickness, 6 mm; interslice gap, 1.5 mm; and matrix, 160×192; b factors, 0 and 800 s/mm^2] or with breath-hold for Toshiba Medical Systems (TR/TE, 2400/70 ms; flip angle, 90°; band width, 1953 Hz/pixel; signal averages, 1; parallel imaging factor, 2; FOV, 35 cm×35 cm; slice thickness, 6 mm; interslice gap, 1.5 mm; and matrix, 160×192; b factors, 0 and 800 s/mm^2). ADC values were calculated from two DW imaging sequences acquired with b=0 s/mm^2 and b=800 s/mm^2. DCE MR imaging was performed before and after administration of gadopentetate dimeglumine (Magnevist, Bayer Schering Pharma, Osaka, Japan) using a transverse three-dimensional (3D) T1-weighted gradient-recalled echo sequence with fat-suppression technique [liver acquisition with volume acceleration (LAVA), GE Healthcare or Quick 3Ds, Toshiba Medical Systems]. The imaging parameters for LAVA were as follows: TR/TE, 4.7/2.2; flip angle, 12°; bandwidth, 62.5 kHz; parallel imaging factor, 2; FOV, 35 cm×35 cm; slice thickness, 2.2–2.5 mm; matrix, 320×192; and acquisition time, 19–20 s. The imaging parameters for Quick 3Ds were as follows: TR/TE, 4.8/1.9; flip angle, 15°; bandwidth, 62.5 kHz; speeder factor, 2; FOV, 35 cm×35 cm; slice thickness, 3.0 mm; matrix, 288×192; and acquisition time, 20 s. DCE MR imaging included corticomedullary phase [25 s or modified scan timing using fluoroscopic triggering (Fluoro Trigger, GE Healthcare, or Visual Prep, Toshiba Medical Systems) or an automated bolus detection algorithm (SmartPrep, GE Healthcare)] and nephrographic (70 s) phase images. Gadopentetate dimeglumine at a dose of 0.1 ml/kg body weight was administered intravenously with a power injector as a rapid bolus at the rate of 3 ml/s, followed by a 30-ml saline flush at a rate of 3 ml/s.

2.3. Image analysis

A retrospective analysis of the imaging was performed for each of the 45 renal tumors by a single reviewer (A.Y., with 6 years of experience in abdominal MR imaging) with no prior knowledge of the diagnoses or clinical information of the patients. The largest region of interest (ROI) that could be accommodated within the largest enhanced portion of the tumor on the corticomedullary phase image on the basis of a visual assessment was placed, and the same region of the ROI was placed on the precontrast and nephrographic phases on DCE MR imaging and DW imaging using the copy and paste method on the PACS system with manual correction where necessary owing to respiratory or patient motion between image acquisitions.